ELSEVIER

Solar Energy Materials & Solar Cells 63 (2000) 197–205

Solar Energy Materials & Solar Cells

www.elsevier.com/locate/solmat

Structure–property relationships in electrochromic WO_3 films deposited by reactive sputtering

X.G. Wang[a,*], Y.S. Jang[a], N.H. Yang[a], Y.M. Wang[a], L. Yuan[b], S.J. Pang[b]

[a]*Department of Vacuum Engineering, Northeastern University of China, P.O. Box 102, Shenyang city 110006, People's Republic of China*

[b]*Beijing Laboratory of Vacuum Physics, Academia Sinica, Beijing 100080, People's Republic of China*

Received 12 June 1996; received in revised form 14 July 1996

Communicated by A. Rooz

Abstract

WO_x electrochromic (EC) films deposited by DC magnetron sputtering technique were investigated by XRD and STM measurements. The reversible microstructure changes of the WO_x film between the bleached and colored EC states were revealed. The study indicates that the amorphous as-deposited WO_x film (a-WO_x) is of amorphous microstructure both in bleached and colored states; however, the crystalline WO_x (c-WO_x) is stoichiometric triclinic lattice WO_3 in bleached state (the lattice parameters: $a = 7.2944$ Å, $b = 7.4855$ Å, $c = 3.7958$ Å, $\alpha = 89.38°$, $\beta = 90.42°$, $\gamma = 90.80°$), and changes into nonstoichiometric tetragonal lattice $WO_{2.9}$ in colored state ($a = b = 5.336$ Å, $c = 3.788$ Å, $\alpha = \beta = \gamma = 90°$). The surface morphologies of the colored WO_x films are very different from those of the bleached WO_x films.

Keywords: Electrochromic; Phases; STM

1. Introduction

Electrochromic (EC) films are widely studied because of their consecutive variable transmittances in luminous wave range. It is difficult to fabricate practical EC devices

* Corresponding author.

E-mail address: wangxg@ele.eng.osaka-u.ac.jp (X.G. Wang)

0927-0248/00/$ - see front matter
PII: S0927-0248(00)00009-X

without understanding thoroughly the EC mechanisms [1,2]. The reversible color changes of bleached and colored states of EC films depend on the film structure. It is reported that the WO_x film's EC effect is caused by the oxygen ion defects in WO_x crystal microstructure, and that the electrons occupy the defect positions forming color centres when electric field is applied to the WO_x films [3,4]. Another report explained EC films mechanism from a band structure theory which depends on film's microstructure [5]. Some other studies with WO_x films have shown the importance of microstructure for EC effect [6–9]. However, in the studies, the microstructure and morphology of reversible EC states of the film have not studied in detail. In this paper, we carried out microstructural and morphology analyses with X-ray diffraction meter (XRD) and scanning tunnelling microscope (STM) for bleached and colored WO_x films. The films were deposited by DC magnetron sputtering technique. The results show that the amorphous WO_x film had amorphous microstructure both in the bleached and colored states; the crystal WO_x undergoes reversible microstructure changes between the bleached and colored states. In addition, the surface morphologies of WO_x films are very different in these two EC states.

2. Experiment

2.1. Sample preparation

WO_x films were obtained by DC magnetron sputtering. The planar target is 99.9% pure tungsten metal with an area of 180 (cm^2). The vacuum chamber was initially evacuated to 5×10^{-3} Pa, and then the pure oxygen and argon gases were pumped through two mass flow controllers separately. The ratio of O_2 to Ar gas was 8 : 2. The total pressure during deposition was 2 Pa and the target power was 375 W. The substrates were SnO_2 : F (FTO)-coated glass plates with a sheet resistance of around 20 Ω/sq. The optical transmittance of the coated glass substrate was 80% in the visible range. The samples area was 1×3 cm^2. The tungsten oxide sputtering rate was kept constant at 1.9 Å/s. The annealing of WO_x film sample was carried out at 200°C for 1 h in vacuum. The as-deposited WO_x film thickness of all samples was 2000 Å.

2.2. Electrochemical and optical properties

Electrochromic WO_x films were cycled electrochemically with platinum and calomel electrodes used as the counter and reference electrodes, respectively, in 0.25 M HCI electrolyte. The WO_x film deposited on FTO(SnO_2 : F) substrates was used as working electrode. On this set up, the as-deposited and annealed WO_x films were cycled between -930 mV and $+800$ mV; the scanning rate was 20 mV/s. After 50 cycles, the sample was withdrawn from the electrolyte, rinsed in distilled water, blow-dried with filtered air, placed in the sample compartment of the spectrophotometer, and subjected to optical measurement. Transmission spectra of the WO_x films in colored and bleached states were recorded on Leng–Guang 721 model

Spectrophotometer in the wavelength range 360 to 800 nm with reference to the FTO(SnO_2 : F)-coated glass plate substrate.

2.3. XRD and STM measurements

The phases and microstructure of initially prepared, annealed WO_x films in different coloration states were investigated by X-ray diffraction using Cu $K_{\alpha 1}$ radiation ($\lambda = 0.1548$ nm). The morphologies of annealed WO_x films in colored and bleached states were studied with scanning tunnelling microscope (CSTM-9000) which operates in air and room temperature conditions. The STM images of bleached and colored as-deposited WO_x and annealed WO_x films, were both obtained after 50 cycles EC reactions with the films and using constant current mode scanning. The STM scanning parameters, including the bias voltage (V_{bia}) and constant tunnelling current (I_{ref}), were changed with the type of WO_x samples at different coloration states. The scanning tips were platinum–iridium alloy wire and sharpened mechanically. Before STM analysis, the samples were treated with the same steps like what we did during the samples preparation for luminous transmittance measurements.

3. Results and discussion

Voltammograms for as-deposited WO_x films and annealed WO_x films are shown in Fig. 1. The Voltammogram of as-deposited WO_x sample (Fig. 1(a)) shows no evidence of oxidation–reduction reaction peaks; but the Voltammogram of annealed WO_x sample (Fig. 1(b)) shows evident oxidation–reduction reaction peaks. This means that the proton insertion and extraction in as-deposited WO_x films during electrochemical cycle have lower resistance than those in the annealed WO_x films. From Fig. 1, no evidence for oxygen or hydrogen evolution is observed. Fig. 2 shows the transmittance spectra of as-deposited and annealed WO_x films in bleached and colored states. From Fig. 2, we can conclude that the as-deposited WO_x films have larger transmittance change between the bleached and the colored states than the annealed WO_x films. Fig. 3 illustrates the XRD pattern of the as-deposited WO_x films in bleached and colored states. Because the tin oxide film, deposited on substrates, is of completely crystal characteristics in its XRD diffraction peaks, the amorphous envelope peak (2θ : 23.15°–33.50°) in Fig. 3, is caused by the as-deposted WO_x films' amorphous propetry. As can be seen in Fig. 3, the as-deposited WO_x films are amorphous (a-WO_x) in both the bleached and the colored states. However, compared with the bleached a-WO_x sample, the colored a-WO_x has a relatively narrow amorphous peak width and more FTO film diffraction peaks. This indicates that the former has better ordering feature than the latter. Fig. 4(a) is the XRD pattern of the annealed WO_x film in the as-prepared state, it is stoichiometric triclinic crystal WO_3 (c-WO_3). The c-WO_3 would change into nonstoichiometric tetragonal crystal $WO_{2.9}$ when colored (see Fig. 4(b)). Soon after, when the colored film is bleached, the film returns to the stoichiometric triclinic c-WO_3 (the XRD pattern is the same as in Fig. 4(a)). This test shows that the microstructural changes for the c-WO_x film are reversible between the

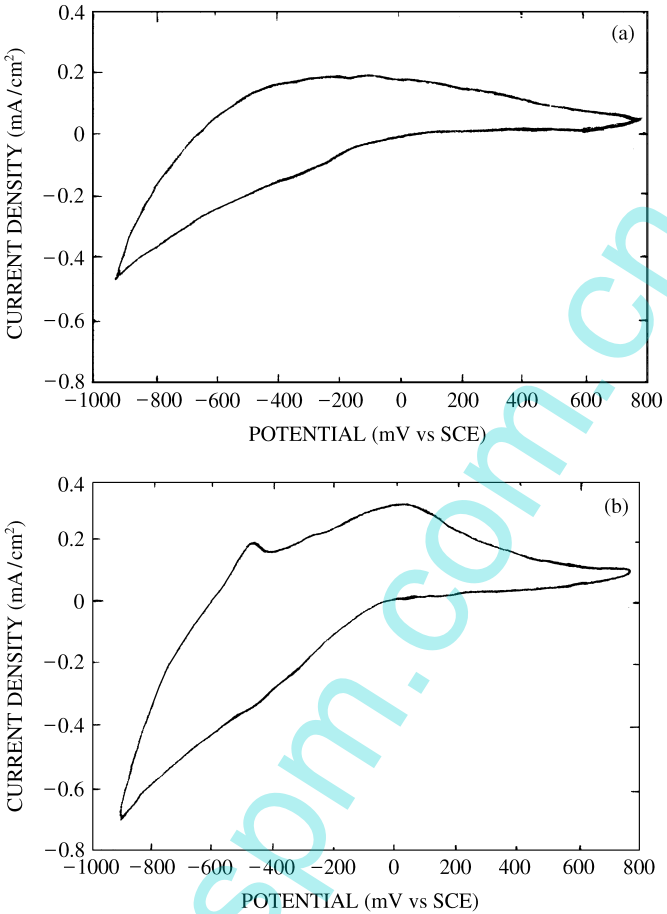

Fig. 1. Cyclic voltammograms of as-deposited and annealed WO_x films in 0.25 M HCI electrolyte at a sweep rate of 20 mV: (a) as-deposited WO_x film area: 0.45 cm^2; (b) annealed WO_x film area: 0.6 cm^2.

bleached and the colored states. With the interplanar distances of our XRD measurements, we calculated the c-WO_x cell lattice parameters and corroborated these with the suggested Perovskite lattice of WO_3 kinds of EC materials [5]. Fig. 5 illustrates the variable unit cell lattice, the parameters are: $a = 7.2944 \pm 0.000027$ Å, $b = 7.4855 \pm 0.000041$ Å, $c = 3.7958 \pm 0.000013$ Å, $\alpha = 89.38°$, $\beta = 90.42°$, $\gamma = 90.80°$ for the bleached state triclinic lattice c-WO_3 film. For the colored-state tetragonal lattice c-$WO_{2.9}$ film the parameters are: $a = b = 5.3358 \pm 0.000076$ Å, $c = 3.7882 \pm 0.000011$ Å, $\alpha = \beta = \gamma = 90°$. The reason for these changes between the colored and the bleached states requires further study. The changes with c-WO_x film were further investigated by STM. Fig. 6 is STM image of the colored state $WO_{2.9}$ film ($V_{bia} = 0.275$ V, $I_{ref} = -1.20$ nA, scanning area is 370×270 nm). Fig. 7 is STM image of the bleached state WO_3 film ($V_{bia} = 0.332$ V, $I_{ref} = -1.17$ nA, scanning

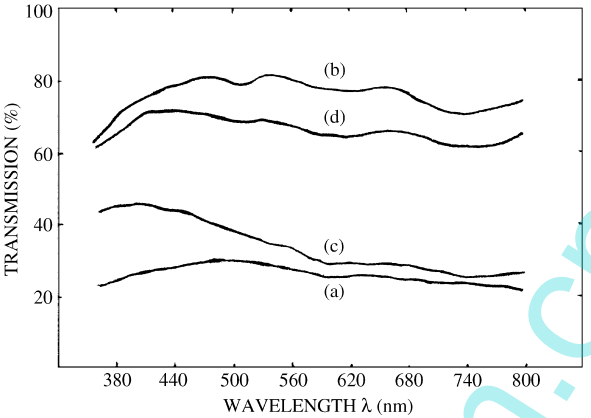

Fig. 2. Spectral transmittances of as-deposited and annealed WO_x films (a) and (b) curves are the transmittances of as-deposted WO_x film in colored and bleached states, (c) and (d) curves are the transmittances of annealed WO_x film in colored and bleached states.

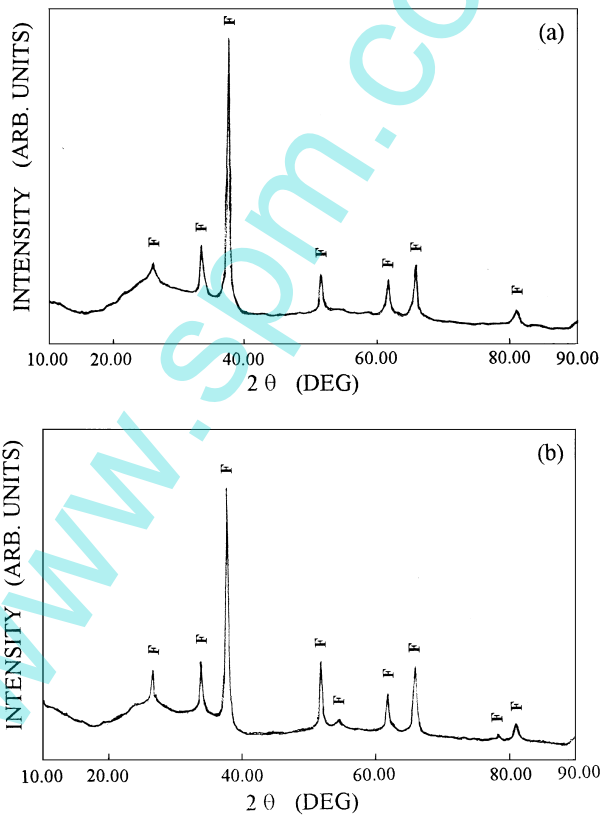

Fig. 3. XRD patterns of as-deposited WO_x film sample: (a) in the original and bleached states, (b) in the colored state. F are the FTO (SnO_2 : F) film peaks.

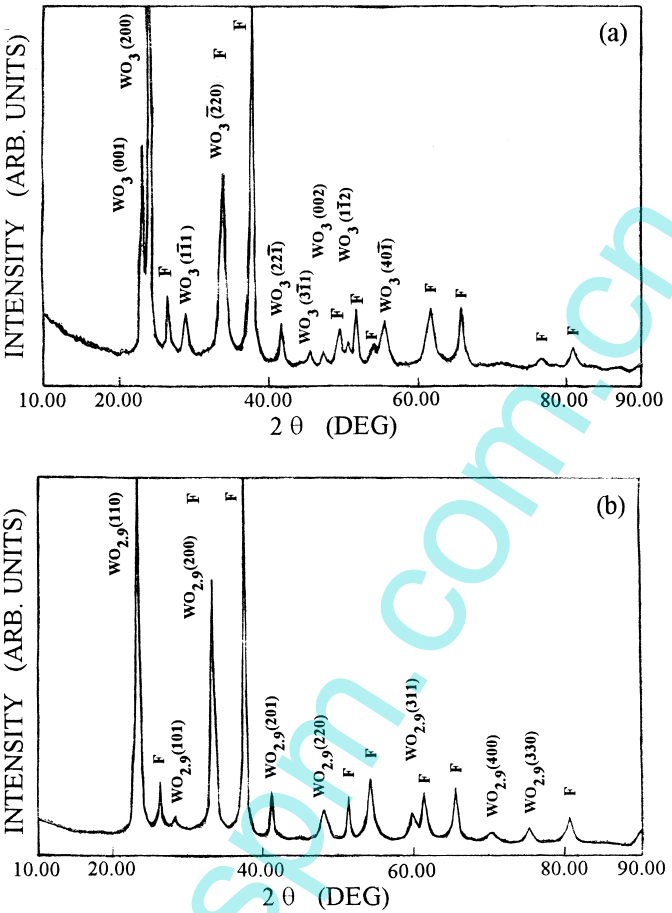

Fig. 4. XRD patterns of annealed WO_x film sample: (a) in the annealed and bleached states, (b) in the colored state. The F are the FTO(SnO_2 : F) film peaks.

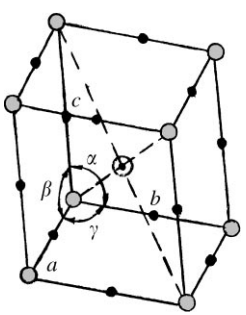

Fig. 5. Illustration of the variable C-WO_x film's cell.

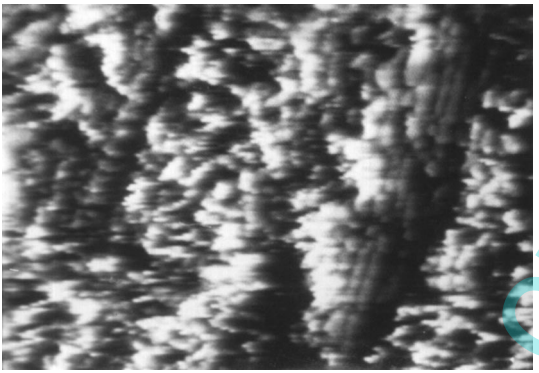

Fig. 6. STM image of the colored state c-$WO_{2.9}$ film, scanning area: 370 nm × 270 nm.

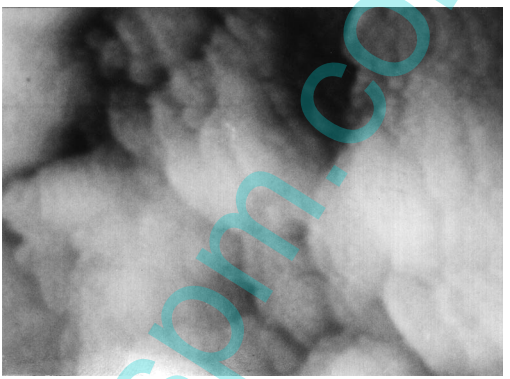

Fig. 7. STM image of the bleached state c-WO_3 film scanning area: 330 nm × 230 nm.

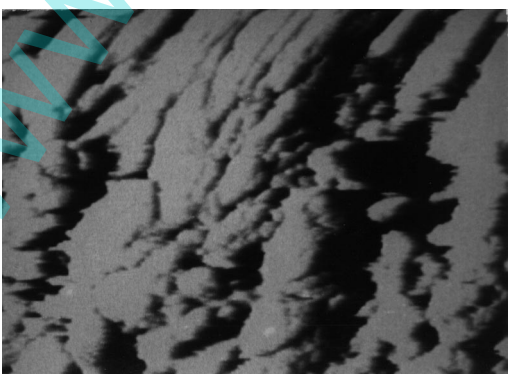

Fig. 8. STM image of the colored state a-WO_x film scanning area: 730 nm × 510 nm.

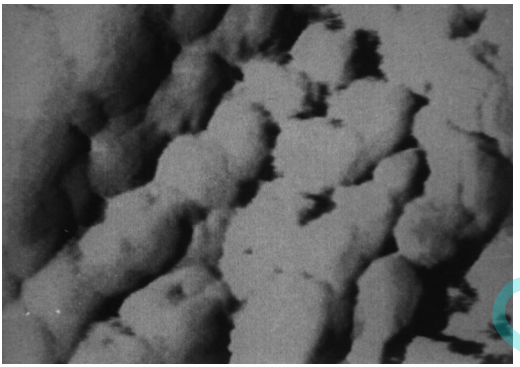

Fig. 9. STM image of the bleached state a-WO_x film scanning area: 800 nm × 550 nm.

area is 330 nm × 230 nm). Figs. 6 and 7 show that the surface morphology of the colored-state c-$WO_{2.9}$ film consists of many very fine grains stacked in a columnar manner and the average grain sizes are about 11 nm; the surface morphology of the bleached state c-WO_3 film consists of a larger fine grains (the average grain sizes are about 30–60 nm) stacked in the same columnar manner. In contrast with c-WO_x film, a-WO_x film was also investigated by STM. Fig. 8 is STM image of the colored state a-WO_x film ($V_{bia} = 0.341$ V, $I_{ref} = -1.12$ nA, scanning area is 730 nm × 510 nm). Fig. 9 is STM image of the bleached state a-WO_x film ($V_{bia} = 0.585$ V, $I_{ref} = -1.04$ nA, scanning area is 800 nm × 550 nm). Figs. 8 and 9 also show that the surface morphology of the colored state a-WO_x film consists of very fine grains stacked in a columnar manner (the average grain sizes are about 20 nm); the surface morphology of the bleached state a-WO_x film consists of relatively larger grains (the average grain sizes are about 110 nm). STM images show that the colored-state WO_x films are more porous than the bleached state WO_x films both for a-WO_x and c-WO_x. The grain-boundaries and the porosity of the films benefit the insertion and extraction of the ions, as reported in Ref. [10]. From our calculation, the unit cell dimension of the bleached state c-WO_3 film is about two times compared with the unit cell dimension of the colored state c-$WO_{2.9}$ film. This change of the crystal lattice must cause changes on the surface microstructure of c-WO_x films, either in the electron density distribution or in the surface morphology.

4. Conclusion

We conclude that the electrochromic property of WO_x films made by DC magnet ron sputtering technique, depends on the microstructure. The as-deposited a-WO_x film remains amorphous in both the colored and the bleached states. The c-WO_x film has a reversible microstructure changes between the colored state (tetragonal lattice) and the bleached state (triclinic lattice). The coordination number x of c-WO_x also changes reversibly (c-WO_x film is of stoichiometric composition WO_3 in bleached

state and nonstoichiometric composition $WO_{2.9}$ in colored state). STM experiments reveal that the bleached WO_x films were composed of many coarse grains (the average grain sizes about 110 nm for a-WO_x and 30–60 nm for c-WO_3 films). In contrast, the colored WO_x films consisted of very fine grains (about 20 nm for a-WO_x and 11 nm for c-$WO_{2.9}$ films) stacked in a columnar manner. The colored-state morphologies in WO_x films were finer grains and more porous than the bleached state morphologies. Further studies on microstructure should be done to obtain more basic information for understanding the coloration mechanism.

Acknowledgements

The first author would like to express gratitude to Mr. G.M. Gao, Mr. H.Q. Yng and Prof. N. Liu for their assistance in STM measurement and their advice.

References

[1] C.M. Lampert, T.R. Omstead, P.C. Yu, Sol. Energy Mater. 14 (1986) 161.
[2] A. Donnadieu, D. Davazoglou, A. Abdellaout, Thin Solid Films 164 (1988) 333.
[3] S.K. Deb, Phil. Mag. 27 (1973) 801.
[4] R.S. Crandall, B.W. Faughnan, Appl. Phys. Lett. 28 (1976) 95.
[5] C.G. Granqvist, Sol. Energy Mater. Solar Cells 32 (1994) 369.
[6] M. Green, X. Karamkang, Displays 10 (1988) 166.
[7] J.P. Cronin, D.J. Tarico, J.C.L. Tonazzi, A. Agrawal, S.R. Kennedy, Sol. Energy Mater. Solar Cells 29 (1993) 371.
[8] S.A. Agnihotry, R. Rashmi, R. Ramchandran, S. Chandra, Sol. Energy Mater. Solar Cells 36 (1995) 289.
[9] T.C. Arnoldussen, J. Electrochem. Soc. 128 (1981) 117.
[10] Q. Zhang, S.A. Wessel, B. Heinrich, K. Colbow, Sol. Energy Mater. 20 (1990) 289.